JACS
JOURNAL OF THE AMERICAN CHEMICAL SOCIETY
Article
pubs.acs.org/JACS

Observation of Photocatalytic Dissociation of Water on Terminal Ti Sites of TiO_2(110)-1 × 1 Surface

Shijing Tan, Hao Feng, Yongfei Ji, Yang Wang, Jin Zhao, Aidi Zhao, Bing Wang,* Yi Luo, Jinlong Yang, and J. G. Hou*

Hefei National Laboratory for Physical Sciences at the Microscale, University of Science and Technology of China, Hefei, Anhui 230026, People's Republic of China

Supporting Information

ABSTRACT: The water splitting reaction based on the promising TiO_2 photocatalyst is one of the fundamental processes that bears significant implication in hydrogen energy technology and has been extensively studied. However, a long-standing puzzling question in understanding the reaction sequence of the water splitting is whether the initial reaction step is a photocatalytic process and how it happens. Here, using the low temperature scanning tunneling microscopy (STM) performed at 80 K, we observed the dissociation of individually adsorbed water molecules at the 5-fold coordinated Ti (Ti_{5c}) sites of the reduced TiO_2 (110)-1 × 1 surface under the irradiation of UV lights with the wavelength shorter than 400 nm, or to say its energy larger than the band gap of 3.1 eV for the rutile TiO_2. This finding thus clearly suggests the involvement of a photocatalytic dissociation process that produces two kinds of hydroxyl species. One is always present at the adjacent bridging oxygen sites, that is, OH_{br}, and the other either occurs as OH_t at Ti_{5c} sites away from the original ones or even desorbs from the surface. In comparison, the tip-induced dissociation of the water can only produce OH_t or oxygen adatoms exactly at the original Ti_{5c} sites, without the trace of OH_{br}. Such a difference clearly indicates that the photocatalytic dissociation of the water undergoes a process that differs significantly from the attachment of electrons injected by the tip. Our results imply that the initial step of the water dissociation under the UV light irradiation may not be reduced by the electrons, but most likely oxidized by the holes generated by the photons.

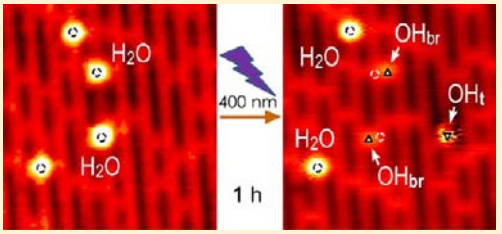

1. INTRODUCTION

The discovery of photocatalytic water splitting on TiO_2[1] has triggered intensive studies on its reaction mechanism[2−7] because of its importance in renewable clean energy applications. However, despite the tremendous efforts, it remains unclear what is the actual initial step for the water splitting reaction.[2,3] Because of the lack of direct experimental evidence, contradicting conclusions have been derived from different models. One of them is about the possible involvement of the photocatalytic reaction. On the basis of the ground-state electronic structure of the water from electron photoemission data,[8,9] it was argued that the adsorbed water molecules at the terminal Ti sites could not be oxidized by the photogenerated holes in the valence band (VB) due to the energy mismatch between the hole and the electronic states of the water,[10−16] whereas the recent density functional theory (DFT) calculations[17,18] suggested that such a mismatch could be overcome by the overpotential created by the photogenerated VB hole in the vicinity of the adsorbed water molecule, resulting in the water photooxidation. Here, we demonstrate for the first time with an atomic resolution that the individually adsorbed water molecules at the terminal Ti sites, that is, the five coordinated Ti (Ti_{5c}) sites, can be dissociated under UV irradiation on the TiO_2 (110)-1 × 1 surface, using an ultrahigh vacuum (UHV) low temperature scanning tunneling microscopy (STM). Our results show that the dissociation of the water can only occur under the irradiation of the UV lights with the wavelengths shorter than 400 nm, which is consistent with the TiO_2 band gap of ∼3.1 eV and indicates clearly the involvement of a photocatalytic dissociation process. As compared to the dissociation process of the adsorbed water molecules through the reduction by the tunneling electrons injected from the STM tip, we found that the photocatalytic dissociation process behaves differently. It allows us to conclude that the initial photocatalytic dissociation of the water should undergo the water oxidation by the photogenerated holes.

2. EXPERIMENTAL SECTION

Our STM experiments were conducted with a low temperature scanning tunneling microscope (Matrix, Omicron) in an ultrahigh vacuum system with a base pressure less than 3×10^{-11} Torr. The measurements were all performed at 80 K. An electrochemically etched polycrystalline tungsten tip was used in the experiment. The rutile TiO_2(110) sample (Princeton Scientific Corp.) was prepared by repeated cycles of ion sputtering (3000 eV Ar^+) and annealing to 900 K with a Ta-foil heater behind the sample. Water (Aldrich, deuterium-depleted, 99.99%) was purified by several freeze−pump−thaw cycles using liquid nitrogen. The water was transferred directly to the TiO_2 surface through a dedicated tube in the chamber. The outlet of the

Received: December 21, 2011
Published: June 1, 2012

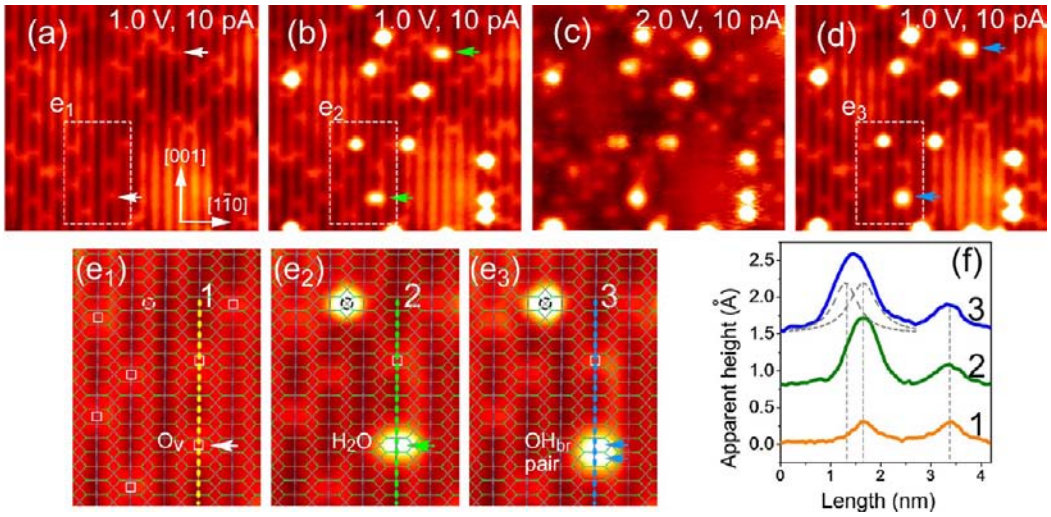

Figure 1. (a,b) STM images before and after H_2O adsorption in situ on TiO_2(110)-1 × 1 (size: 12.3 × 11.2 nm^2, imaged at 1.0 V and 10 pA, 80 K). (c,d) Consecutively acquired STM images at 2.0 and 1.0 V, respectively. White arrows, O_V sites; green arrows, molecular H_2O at O_V sites; blue arrows, OH_{br} pairs. (e_1−e_3) Magnified images (3.7 × 4.6 nm^2) marked by rectangles, superposed with structural model of TiO_2 surface. ○, water adsorption sites at Ti_{5c}; □, O_V site. (f) Line profiles along lines 1−3, respectively, separated vertically by 0.75 Å for clarity. The profile for OH_{br} pair (in line 3) can be fitted by two peaks.

tube was only about 5 mm from the TiO_2 surface. This method minimized the background water in the chamber and helped to keep the sample surface almost unchanged in the dark for about 9 h (Supporting Information Figure S1). This benefits from the microscope covered with the two-levels cooling shield, which acts as a trapping pump and may keep a much higher vacuum in the space of the microscope at 80 K. With this experimental condition, we were able to keep quite a few contaminated adsorbates that might further adsorb on the surface during the light irradiation measurements. The dosing amount was not able to be monitored by the ion gauge; instead, we directly determined the coverage by the STM images. During the water dosing, the sample was maintained at 80 K.

The light irradiation measurements were performed with different wavelengths by using light sources of mercury−xenon lamp (Hammatsu, L2423, equipped with bandpass filters: centered at 400 and 440 nm with bandwidths of 40 and 20 nm, respectively; a quartz convex lens is used to ensure almost parallel incident light), Nd:YAG laser (Spectra-Phyiscs, Pro-250; repetition, 10 Hz; duration, 10 ns; for wavelengths of 532, 355, and 266 nm), and excimer laser (Coherent Inc., COMPexPro 201, ArF; repetition, 4 Hz; duration, 20 ns, for wavelength of 193 nm). A specially coated sapphire window (VG Scienta) was employed for 193 nm UV light with 90% transmission. The light spots had a size of about 10 mm in diameter on the surface centered at around the tip position, which had been aligned with a screen mounted at the sample site. The angle between the incident light and the sample surface was about 30°. The light intensity was measured by a detector (OPHIR, PD300-UV-193) with the normal incidence at the outside of the chamber in front of the window. These nominal intensities used in the experiment were mainly 1.0 mW/cm^2 for the laser lights (at 532, 355, 266, and 193 nm), 5.1 mW/cm^2 for the light of 400 ± 20 nm, and 2.2 mW/cm^2 for the light of 440 ± 10 nm. Because the detector was not able to be mounted at the sample site, we could just calibrate the light intensities in the ambient condition. The intensities were measured at a distance (including the window) similar to the one from the window to the sample in the chamber. The intensity is found to be reduced by about 10% for the laser lights, and 30% for the lights of the mercury−xenon lamp (400 ± 20 and 440 ± 10 nm) because of its poor collimation even after a lens is adopted. Taking into consideration the incident angle, the calibrated light intensities on the sample surface were about 0.45 mW/cm^2 for the laser lights, 1.8 mW/cm^2 for the 400 ± 20 nm light, and 0.8 mW/cm^2 for the 440 ± 10 nm light.

During the light irradiation, the tip was retracted back about 25 steps (each step is about 400 nm) from the surface, so the tip−sample distance was estimated to be about 10 μm, which could avoid the shadow of the STM tip on the measured area of the sample surface. At 80 K, the thermal drift between the tip and the sample surface was typically less than 10 nm/h, which allowed us to find the same areas that had been characterized. We always compared the areas before and after the light irradiation to trace any changes on the surface.[19]

3. RESULTS

3.1. Adsorption Behavior of Water at 80 K. Figure 1a and b gives a pair of representative images before and after the water dosing within the same area on the TiO_2(110)-1 × 1, acquired under the conditions of 1.0 V (positive sample bias with respect to the tip) and 10 pA at 80 K. The concentration of the bridge-bonded oxygen vacancies (O_V) is about 0.08 ML (1 ML = 5.2 × 10^{14} cm^{-2}). The water coverage is about 0.02 ML. By counting thousands of adsorbed water molecules, it is found that only 9% water molecules appear at the O_V sites, and 91% adsorbed water molecules at the Ti_{5c} sites. Similar distribution was obtained for the water coverage ranging from 0.02 to 0.05 ML. Unlike the diffusive water molecules at elevated temperatures,[20] it is observed that the adsorbed water molecules are quite immobile at 80 K, which makes it easy to trace any possible reactions under UV irradiation.

Figure 1c and d shows the consecutively acquired images at 2.0 and 1.0 V, respectively. Although the images acquired at 2.0 V show some noticeable feature changes for the water molecules at the Ti_{5c} sites (Figure 1c), when the voltage goes back to 1.0 V, the images can always be recovered (Figure 1d). It indicates that the adsorbed water molecules at the Ti_{5c} sites are not dissociative when the applied voltage is lower than 2.0 V (with a set point current of 10 pA). As for the feature changes at higher voltages, one plausible explanation might be the involvement of the oscillation of the water molecules induced by the tip.

It is noted that the molecules at the O_V sites have already been dissociated to pairs of hydroxyl species, that is, OH_{br}, after scanning once at 1.5 V (not shown). The areas marked by the rectangles are correspondingly magnified in Figure 1e_1−e_3, with

dx.doi.org/10.1021/ja211919k | J. Am. Chem. Soc. 2012, 134, 9978−9985

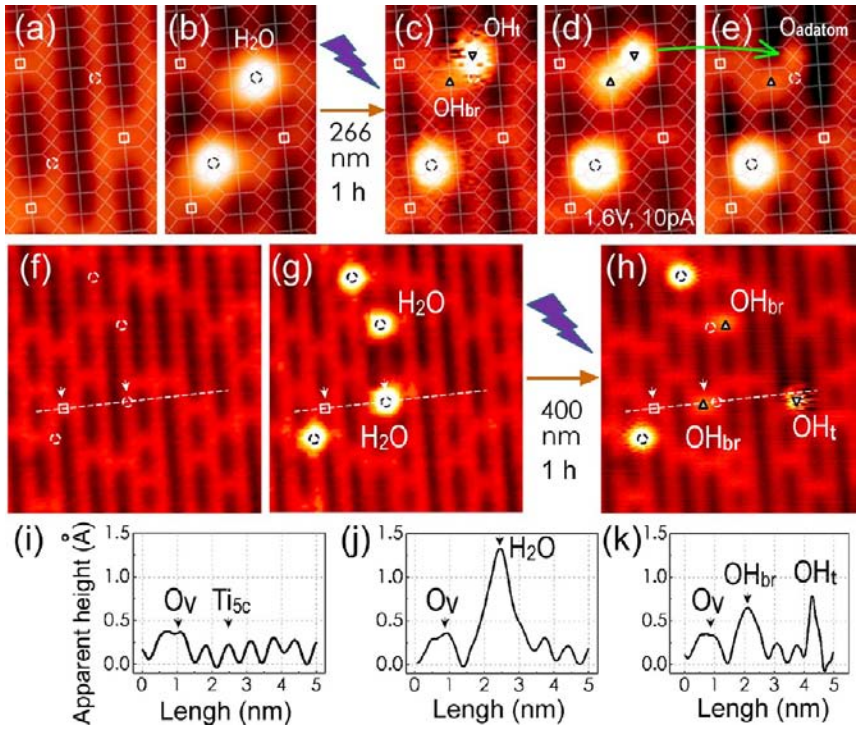

Figure 2. (a,b) STM images (size: 1.9 × 2.9 nm^2, imaged at 1.0 V and 10 pA, 80 K) before and after water dosing. (c) Image after 266 nm UV irradiation for 1 h (Nd:YAG laser; repetition, 10 Hz; duration, 10 ns; nominal intensity, 1 mW/cm^2). (d) Image acquired consecutively at 1.6 V and 10 pA. (e) Image (at 1.0 V and 10 pA) showing the further dissociation of the OH_t to an O_{ad} at the Ti_{5c} site by applying a voltage pulse of 2.4 V. (f–h) Another set of images (6.3 × 6.6 nm^2, imaged at 1.0 V and 10 pA, 80 K) showing the dissociation of water molecules under the 400 nm UV irradiation for 1 h (mercury–xenon lamp from Hammatsu, L2423, with a bandpass filter centered at 400 nm and bandwidth of 40 nm, nominal intensity: 5.1 mW/cm^2). (i–k) Line profiles along the lines in (f), (g), and (h), respectively. White ○, adsorption sites of water at Ti_{5c}; black ○, molecular water at Ti_{5c}; □, O_V sites; △, OH_{br}; ▽, OH_t.

the superposed structural model. It can be seen that the water molecule at the O_V site becomes expanded, occupying two lattice sites in the bridging oxygen row (Figure 1f). This is consistent with the well-characterized feature of the thermally driven dissociation of the water molecules at the O_V sites at elevated temperatures.[4,7,21−28] In our measurements, the adsorbed water molecules at the O_V sites may be dissociated after several scanning cycles at 1.0 V and 10 pA at 80 K (Supporting Information Figure S2). However, at the bias voltages higher than 1.5 V, the voltage-dependent dissociation behavior typically occurs for the water molecules at the O_V sites. It suggests that the tip-induced dissociation could be an additional process for the water molecules at the O_V sites, to form the OH_{br} pairs at 80 K. It should be mentioned that under the typical experimental conditions of 1.0 V and 10 pA, the OH_{br} pairs remain intact during the measurements.

On the basis of our measurements, we have found that the imaging condition of 1.0 V and 10 pA allows us to obtain good images without the risk of tip-induced dissociation of the water at the Ti_{5c} sites. The STM measurements described in the following sections were performed under such a condition, if not specified.

3.2. Dissociation of the Water Molecules Adsorbed at the Ti_{5c} Sites under UV Irradiation. We now turn our attention to the photocatalytic reaction of the water molecules adsorbed at the Ti_{5c} sites. The results presented in Figure 2 provide direct evidence that the adsorbed molecules at the Ti_{5c} sites can be dissociated under UV irradiation. In Figure 2a–c, it can be seen that one of the water molecules disappears from its original Ti_{5c} site after the 266 nm light irradiation for 1 h. Meanwhile, a less protruded spot at the adjacent O_{br} and a fuzzy spot at the nearby Ti_{5c} site (from the original water adsorption site by one lattice distance) simultaneously show up. This can certainly be attributed to the dissociation of the water molecule at the Ti_{5c} site under UV irradiation. In the consecutively acquired image at 1.6 V and 10 pA (Figure 2d), the fuzzy spot becomes more smooth, and it can be further dissociated to an O adatom by applying a voltage pulse of 2.4 V (Figure 2e). Such a dissociation process is a result of the inelastic electron tunneling, similar to what was observed before for the tip-induced desorption of hydrogen from OH_{br}.[28,29] Therefore, we may attribute the fuzzy spot to hydroxyl species, OH_t, at the Ti_{5c} sites, and then the less protruded spot to OH_{br} species as the result of the hydrogen transferring to the adjacent O_{br} site. It is noticed that the OH_t species were observed before,[30,31] but did not show such a fuzzy feature. We have therefore carried out a systematic study and found that the image of OH_t is voltage-dependent (see Supporting Information Figure S3). It was observed that the OH_t species are quite immobile even imaged at bias voltages of 1.5−1.8 V and at 300 K.[31] Thus, we tend to believe that the fuzzy feature can be associated with the local change of the OH_t because in our measurements we typically observed the fuzzy feature at much lower bias voltages of 0.7−1.0 V and at a much lower temperature of 80 K. In other words, the swing of the OH bond leads the fuzzy feature, and the swing rate is increased with the increase of the applied bias voltage. When the swing of the OH bond is too fast and exceeds the bandpass of the preamplifier of our STM instrument (the bandwidth of the preamplifier used in this experiment is about 800 Hz), the recorded image can

dx.doi.org/10.1021/ja211919k | J. Am. Chem. Soc. 2012, 134, 9978−9985

only reflect the averaged signals (say at 1.6 V and 10 pA). This is consistent with the observation that the image is no longer fuzzy at 1.6 V. All of these findings can thus well explain the difference between our observations and reported in the literature.[30,31] Obviously, one can use such a unique fuzzy feature to identify the OH_t species. It is helpful to mention that similar results have been obtained for a melamine molecule adsorbed on Cu(100) surface, in which the swing of a NH bond generates similar behaviors.[32] We refer to that work for detailed theoretical analysis.

Similar results were obtained under the irradiation of UV lights with different wavelengths. Figure 2f–h show another set of images under the irradiation of 400 nm light (mercury–xenon lamp, with a band-pass filter centered at 400 nm and bandwidth of 40 nm). It is observed that OH_{br} is always present at the adjacent O_{br} accompanying the water dissociation under UV irradiation, as shown in Figure 2h. Two water molecules are dissociated in the frame of Figure 2h, but only one OH_t can be observed at a Ti_{5c} site away from the original place by several lattice distance over the O_{br} rows. The line profiles shown in Figure 2i–k give the apparent height of these H_2O, OH_t, and OH_{br} species, which have also been further confirmed by the tip manipulation (Supporting Information Figure S4).

Our results demonstrate that under the UV light irradiation the water molecules at the Ti_{5c} sites can be dissociated into two types of OH species. One type is always present as OH_{br} at the adjacent O_{br} cites, and the other type either desorbs from the surface or adsorbs as OH_t. The adsorbed OH_t species generally occur away from the sites at which the water molecules originally stayed.

3.3. Dependence of Water Dissociation on Wavelength. We further examined the effect of the light wavelength on the dissociation probability. As shown in Figure 3a–c, we give a relatively large area to illustrate the results for the sample under the irradiation of 400 ± 20 nm light with a nominal light intensity of 5.1 mW/cm^2 for 1 h. In this area, there are three dissociated water molecules, as marked by the dashed rectangles in images a–c of Figure 3, which are correspondingly magnified in Figure 3a_1–a_3, b_1–b_3, c_1–c_3. In Figure 3c_1, a fuzzy OH_t can be observed accompanying the dissociation of one water molecule. In the other two cases of the water dissociation shown in Figure 3c_2 and c_3, OH_t species do not occur. In all of these cases, the OH_{br} species are present at the adjacent O_{br} sites. One may note that there are some adsorbates or defects before the water dosing in Figure 3a, marked by the dashed green circles. After the light irradiation, these species do not show an obvious change (Figure 3c), which should thus not affect the results for the water dissociation. In the same run, we acquired four other sets of images from different areas nearby. With a total number of about 650 adsorbed water molecules at the Ti_{5c} sites, 11 dissociation events were observed after the 400 nm light irradiation, which leads to the dissociation probability of about 1.7%.

Another set of representative images of the sample irradiated under 355 nm light for 2 h is given in Figure 3d–f. It can be seen that two water molecules are dissociated in the frames marked by the rectangles, which are also correspondingly magnified in Figure 3d_4–d_5, e_4–e_5, f_4–f_5. In both cases, the OH_t are not produced, while the OH_{br} species still occur at the adjacent O_{br} sites (Figure 3f_4–f_5). The total number of the adsorbed water molecules at the Ti_{5c} sites was 217 from six different areas in the run, and eight dissociated molecules were

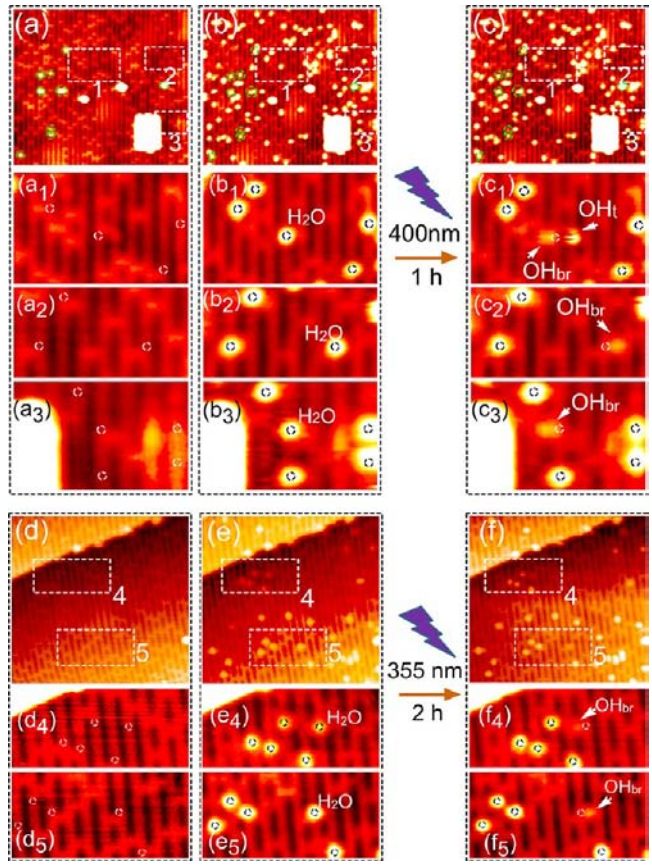

Figure 3. (a–c) Large-scale images (23.0 × 20.5 nm^2) before water dosing, after water dosing, and after 400 ± 20 nm light irradiation for 1 h (nominal intensity of 5.1 mW/cm^2), respectively. The dashed green circles mark the preexisted adsorbates or defects. (a_1–c_1) Magnified images of frame 1 (6.5 × 3.9 nm^2), (a_2–c_2) frame 2 (5.2 × 2.8 nm^2), and (a_3–c_3) frame 3 (3.9 × 2.7 nm^2). (d–f) Another set of images (17.5 × 16.6 nm^2) before water dosing, after water dosing, and after 355 nm light irradiation (nominal intensity of 1.0 mW/cm^2) for 2 h, respectively. (d_4–f_5) Magnified images of frame 4 (6.8 × 3.0 nm^2) and (d_5–f_5) frame 5 (7.1 × 3.5 nm^2). Imaged at 1.0 V and 10 pA, at 80 K.

observed. It corresponds to the dissociation probability of about 3.7% in this run.

For the sample under the irradiation of 532 nm light (see Supporting Information Figure S5), however, all water molecules remain unchanged. We performed similar measurements on more than five runs and were unable to observe any dissociation events for more than 1500 water molecules.

The measurements for the different wavelengths were mainly performed with the nominal intensity of 1 mW/cm^2 for the laser lights (about 0.45 mW/cm^2 on the surface by calibration) and 5.1 mW/cm^2 (1.8 mW/cm^2 on the surface by calibration) for the 400 ± 20 nm light. Figure 4a demonstrates the dissociated fraction of the adsorbed water molecules as a function of the irradiation time at various wavelengths. It is important to mention that the dissociation events could be only observed when the wavelength of the light is shorter than 400 ± 20 nm, which accords well with the band gap of 3.1 eV for the rutile TiO_2. Our observations here lead to a conclusion that the dissociation of water at the Ti_{5c} sites should be a photocatalytic process.

It should also be noticed that, although we do observe the water dissociation, the dissociation probabilities are very low, typically 2% and 4% after UV irradiation for 1 and 2 h,

dx.doi.org/10.1021/ja211919k | J. Am. Chem. Soc. 2012, 134, 9978–9985

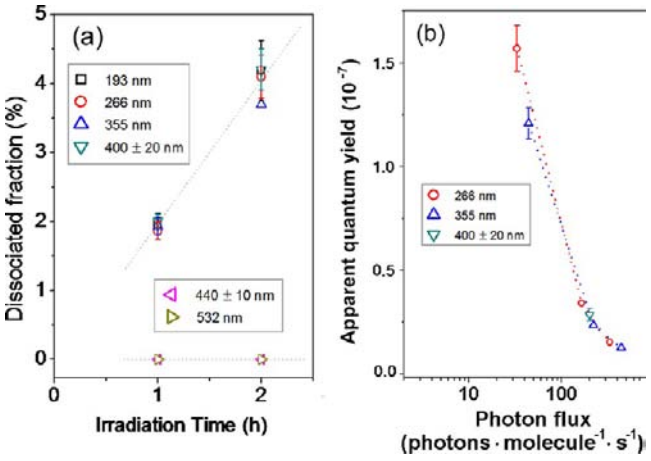

Figure 4. (a) Plot of the dissociated fraction of the water molecules at the Ti_{5c} sites as a function of the irradiation time. The vertical error bars give the standard deviation of the data in more than three runs (for each point, the accumulated total number of water molecules was about 1000 or more). For 355 nm irradiation for 2 h, only one run was performed (217 molecules). The gray dotted lines are to guide the eyes only. (b) Plot of the apparent quantum yield as a function of the photon flux.

respectively. Moreover, the dissociation probability does not show obvious dependence on the wavelength in the range of 400−193 nm with the given intensities. In other words, once the energy of the light is larger than the band gap of the TiO_2, the dissociation event occurs with almost similar probability in our measurements.

Because of the rather low dissociation probability, the fluctuation in the measurements might be relatively large. For instance, the dissociation events could be observed in some areas (typically within 20 × 20 nm^2), but might not be in other nearby areas within the same run. One way to enhance the dissociation probability would be to increase the intensity of the light. We made several runs with higher nominal intensities of 5 and 10 mW/cm^2 using the lights of 266, 355, and 532 nm, respectively. It is quite unexpected to see that the dissociation probability barely changes over the intensity range. It is noted that the irradiation with the 532 nm light cannot trigger the water dissociation even with higher intensity up to 10 mW/cm^2. However, we have also found that with a lower nominal intensity of 0.1 mW/cm^2 for both 266 and 355 nm light, and 0.7 and 1.2 mW/cm^2 for the light of 400 nm, it is impossible to detect any dissociation events after the irradiation for 2 h. This implies that a relative high light intensity is needed for the water dissociation.

We obtain the apparent quantum yield as a function of the photon flux, and the results are plotted in Figure 4b. The apparent quantum yield is defined as the dissociated events over the total number of incident photons. The photon flux is given in the unit of photons·$molecule^{-1}$·s^{-1}. Considering the narrow variation of the water coverage in the range of 0.02−0.05 ML, we have taken the result for an averaged coverage of 0.035 ML, corresponding to a value of 1.8 × 10^{13} molecule/cm^2. It can be seen that with the increase of the calibrated light intensity, the number of photons per molecule increases from several to several hundred, varying with the wavelength of the incident light. This is consistent with previous experimental observations that show the absorption coefficient of the light at 400 nm is much smaller than that of the shorter wavelength lights.[33,34] It is noted that with the water coverage higher than 0.1 ML, the quality of the images does not allow us to precisely determine whether the reaction takes place or not. We have also observed that the concentration of O_V varies in the range of 0.08−0.12 ML; however, its influence on the water dissociation probability is not identified yet. Because of the low water coverage, the dissociation events can be detected only when the photon flux reaches a certain value. As shown in Figure 4b, the apparent quantum yield demonstrates a monotonic decrease, indicating that the increase of the incident photons does not produce extra dissociation events. Our observation is consistent with the results that in TiO_2 nanoparticle photocatalyst, four photons per particle are already sufficient to reach the saturated quantum yield of water splitting.[3,35,36]

Although we have tried minimizing the hydroxyl species on the surface, we can still observe some preexisted OH_{br} species, with a typical number of 1−10 within an area of about 20 × 20 nm^2 before the water adsorption. These OH_{br} species were mainly produced in the preparation chamber or during the sample transferring. Once the samples were mounted at the cryostat of the microscope covered with the cooling shield, no any additional contaminations could be observed. These preexisted OH_{br} species were quite stable and immobile during the light irradiation and behaved similar to the OH_{br} pairs from the dissociative water at the O_V sites (Supporting Information Figure S2). Therefore, we believe that these preexisted OH_{br} species do not affect the observed water dissociation events in our experimental condition.

3.4. Tip-Induced Dissociation of the Water Molecules Adsorbed at the Ti_{5c} Sites. As a comparison, we performed the experiment by applying voltage pulse on the water molecules at the Ti_{5c} sites. The tip-induced dissociation of the water can be observed at much higher positive bias voltages. As shown in Figure 5a−c, by applying voltage pulse of 2.4 or 2.8 V on an adsorbed water molecule at the Ti_{5c} site, its image can be changed either to a less pronounced spot or to a fuzzy spot at exactly the same site where the water molecule was originally adsorbed. The less pronounced spot can be assigned to an O adatom (O_{ad}),[37−39] due to the direct removal of the

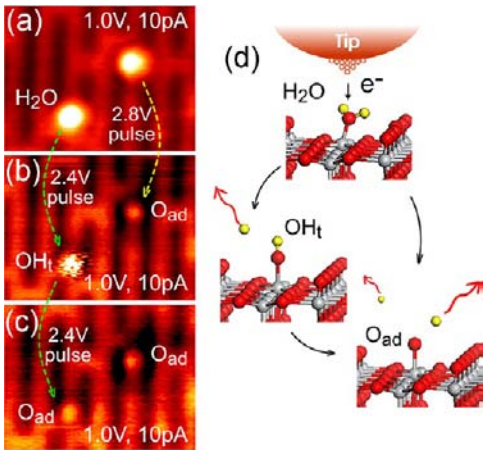

Figure 5. (a−c) STM images (size: 3.9 × 3.0 nm^2, imaged at 1.0 V and 10 pA, 80 K) of the tip-induced water dissociation to produce OH_t or oxygen adatom (O_{ad}) under different applied bias voltages. (d) Schematic drawings showing structural models of different processes of the tip-induced water dissociation.

dx.doi.org/10.1021/ja211919k | J. Am. Chem. Soc. 2012, 134, 9978−9985

two hydrogen atoms from the water molecule, and the fuzzy spot to an OH_t species as a result of the removal of a single hydrogen atom. The latter can also be further dissociated to an O_{ad} (Figure 5c). The OH_t produced by the tip also shows the voltage-dependent features, similar to the ones produced under UV irradiation discussed above, which further confirms our assignment. The tip-induced dissociation processes are schematically illustrated in Figure 5d, where one or both of the hydrogen atoms can be removed. We also applied negative sample bias to carry out a similar manipulation. However, no dissociation event was observed even when the negative voltage pulse (negative sample bias with respect to the tip) was set to −4.0 V. Our observations indicate that the injected tunneling electrons play a dominant role in the dissociation of the water molecules. It is consistent with what was reported before for the dissociation of H_2O on MgO[40] or CO_2 on $TiO_2(110)$[41,42] by applying a relatively high bias voltage. Such a process partly mimics the reduction of adsorbed water molecules through attachment of electrons injected by the STM tip. In the tip-induced water dissociation process (Figure 5b and c), the reduction through the attachment of electrons always leads to the removal of one or two hydrogen atoms from the water molecule, only leaving an OH_t or an O adatom at the exact site that the water molecule originally stayed. This is quite different from the water dissociation under UV irradiation, which suggests that the dissociation of the water under UV irradiation is a process completely different from the water reduction by the injected electrons.

4. DISCUSSION

On the basis of what we have observed, the possible photocatalytic dissociation process of the water under UV irradiation is schematically illustrated in Figure 6. In this

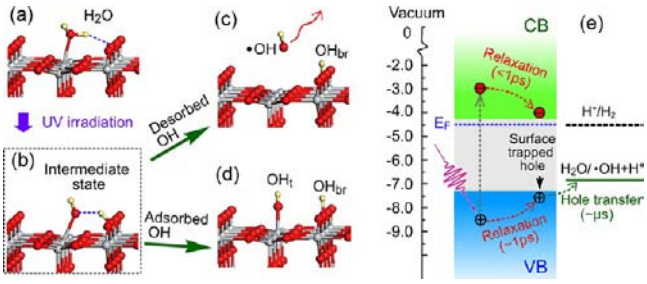

Figure 6. (a) Structural model of water at a Ti_{5c} site under UV irradiation. (b) Possible intermediate state under UV irradiation. (c) Dissociation of the adsorbed water molecule into OH_{br} and desorbed •OH, or (d) OH_{br} and adsorbed OH_t at a Ti_{5c} site. (e) Energy diagram and relaxation time scales of the photogenerated electron−hole pair by photon with energy larger than the TiO_2 bandgap (refs 11, 14, 48−52).

reaction step, one of the hydrogen atoms is transferred to the adjacent bridge oxygen (Figure 6b), forming an OH_{br}. The left OH species may either desorb from the surface or adsorb as an OH_t at a certain Ti_{5c} site (Figure 6c and d). Our measurements show about 80% OH species to desorb from the surface. These desorbed OH species could correspond to the observed gas-phase •OH radicals in previous spectroscopic studies.[43−46] The OH_t species are often observed at Ti_{5c} sites away from where the water was originally. It could suggest that the OH_t species might be diffusive under UV irradiation, or it was generated through the "cannon-ball"-like mechanism as observed for the dissociation of a chlorine molecule on $TiO_2(110)$.[47] Considering the fact that most of the OH species desorb from the surface and the OH_t species occur away from the original sites and even over several oxygen rows, the water dissociation may most likely follow the "cannon-ball"-like mechanism in the photocatalytic process because of the large exothermically dissociation energy generated by UV irradiation. However, because there are too few OH_t species left on the surface, it is not possible to obtain the statistical distribution of OH_t positions. In contrast, it is noted that the OH_{br} species are quite inert and immobile under UV irradiation.

Figure 6e gives the energy diagram and the relaxation time scales.[11,14,48−52] Because some data for the solid−vacuum interface are not available, we adopt the results for the solid−liquid interface instead. When the photon energy is larger than the band gap energy of TiO_2, it can generate holes at a level below the VB maximum (deep holes) and electrons at a level higher than the CB minimum (hot electrons).[3] These photogenerated hole−electron pairs relax to the respective band edges before they can reach the reactants.[53] It is known that the relaxation of the deep holes to the VB maximum is in the time scale of a few picoseconds,[2,14,48] while the transfer of the surface trapped holes to the adsorbed water molecules is around several microseconds.[49] In comparison, the relaxation of the hot electrons is in the scale of several tens to hundred femtosecond,[50−52] and the transfer of the trapped electrons to the adsorbed water molecules is on the much longer time scale around several tens to hundreds microsecond.[49] The fast relaxation of the deep holes to the VB maximum and the hot electrons to the CB minimum may cause the reactants to dominantly get the relaxed carriers from the band edges. This might explain the observations that the dissociation probability is independent of the UV wavelength (Figure 4a).

Because the transfer rate for the holes to the water molecules is faster by 1 or 2 orders of magnitude than that for the electrons to the water molecules, it is reasonable to believe that the reaction of the holes with the water molecules should be more favorable and dominant in the photocatalytic dissociation reaction.[2] Moreover, for the tip-induced water dissociation, the electron injection is known to play the dominant role, which results in the removal of the hydrogen atom(s) (Figure 5). This is very different from the photocatalytic reaction, in which the OH_{br} is formed at the neighboring site (Figure 2) and no oxygen adatom is generated. On the basis of these facts, the photocatalytic dissociation of the water observed in this study should not be a reduction, but an oxidation reaction that could be described as

$$H_2O + h^+ \rightarrow \bullet OH + H^+ \quad (1)$$

where h^+ refers to the photogenerated hole by photon ($h\nu \xrightarrow[>3.1eV]{TiO_2} h^+ + e^-$) in the TiO_2 VB.

It was suggested that the photogenerated VB holes on TiO_2 surfaces do not have the potential energy needed to oxidize either adsorbed water or OH^- groups in solution,[10−13,44] because the photogenerated VB holes rapidly relax to the TiO_2 VB maximum,[14−16] and the highest occupied molecular orbitals of the adsorbed water molecules are energetically much lower than the TiO_2 VB maximum.[8] This picture was based on the ground-state electronic structure of the system and is obviously not supported by our observations. The photoexcitation can generate the hole−electron pair, and it can also alter the position of the molecular orbitals.[17,18,54]

dx.doi.org/10.1021/ja211919k | J. Am. Chem. Soc. 2012, 134, 9978−9985

There were suggestions that the oxidation of the water could be initiated by the •OH radicals[10,12] or the nucleophilic attack,[11,13] but not due to the reaction of the holes with the adsorbed water and/or OH^- species. The source of •OH radicals was then suggested to be from several different processes, like the reaction between the holes and the O_s^{2-} terminal ions,[12] electroreduction of dissolved oxygen molecules with CB electrons,[55] or direct photolysis of photogenerated H_2O_2.[56] In our measurements under the UHV condition, these situations can be excluded, and the •OH radicals can only be generated from the dissociation of the individually adsorbed water molecules. Our experimental results clearly conclude that the initial reaction step can proceed through the photocatalytic reaction, and most likely through photooxidation by the holes, which disproves the hypothesis that the water at the terminal Ti sites cannot be photooxidized.[12] Of course, it is highly possible that in aqueous solutions some other processes[11−13,55] could occur in the successive reactions or even simultaneously during the direct photooxidation of water.

5. CONCLUSIONS

We have provided atomically resolved evidence that individual water molecules at Ti_{5c} sites of reduced $TiO_2(110)$-1 × 1 surface can be photocatalytically dissociated under UV irradiation. In the UHV conditions, it is revealed that this dissociation process can be the initial reaction step in the water splitting reaction sequence. Unlike the tip-induced dissociation process, we suggest that this photocatalytic reaction should be an oxidation process triggered by the photogenerated holes. The identification of this initial reaction step is original and significant, which sheds new light on the understanding of the whole photocatalytic water splitting reaction chain.

■ ASSOCIATED CONTENT

Supporting Information

More detailed experimental results and complete ref 19. This material is available free of charge via the Internet at http://pubs.acs.org.

■ AUTHOR INFORMATION

Corresponding Author

bwang@ustc.edu.cn; jghou@ustc.edu.cn

Notes

The authors declare no competing financial interest.

■ ACKNOWLEDGMENTS

This work was supported by NBRP (grants 2011CB921400 and 2010CB923300) and NSFC (grants 9021013, 10825415, 10874164, 20925311, 21003113, 21121003), China.

■ REFERENCES

(1) Fujishima, A.; Honda, K. *Nature* **1972**, *238*, 37−38.
(2) Henderson, M. A. *Surf. Sci. Rep.* **2011**, *66*, 185−297.
(3) Fujishima, A.; Zhang, X.; Tryk, D. *Surf. Sci. Rep.* **2008**, *63*, 515−582.
(4) Dohnálek, Z.; Lyubinetsky, I.; Rousseau, R. *Prog. Surf. Sci.* **2010**, *85*, 161−205.
(5) Thompson, T. L.; Yates, J. T. *Chem. Rev.* **2006**, *106*, 4428−4453.
(6) Diebold, U. *Surf. Sci. Rep.* **2003**, *48*, 53−229.
(7) Hammer, B.; Wendt, S.; Besenbacher, F. *Top. Catal.* **2010**, *53*, 423−430.
(8) Krischok, S.; Höfft, D.; Günster, J.; Stultz, J.; Goodman, D. W.; Kempter, V. *Surf. Sci.* **2001**, *495*, 8−18.
(9) Kurtz, R. L.; Stockbauer, R.; Madey, T. E.; Roman, E.; Desegovia, J. L. *Surf. Sci.* **1989**, *218*, 178−200.
(10) Salvador, P. *Prog. Surf. Sci.* **2011**, *86*, 41−58.
(11) Imanishi, A.; Okamura, T.; Ohashi, N.; Nakamura, R.; Nakato, Y. *J. Am. Chem. Soc.* **2007**, *129*, 11569−11578.
(12) Salvador, P. *J. Phys. Chem. C* **2007**, *111*, 17038−17043.
(13) Nakamura, R.; Nakato, Y. *J. Am. Chem. Soc.* **2004**, *126*, 1290−1298.
(14) Grela, M. A.; Brusa, M. A.; Colussi, A. J. *J. Phys. Chem. B* **1997**, *101*, 10986−10989.
(15) Tamaki, Y.; Furube, A.; Murai, M.; Hara, K.; Katoh, R.; Tachiya, M. *J. Am. Chem. Soc.* **2006**, *128*, 416−417.
(16) Bahnemann, D. W.; Hilgendorff, M.; Memming, R. *J. Phys. Chem. B* **1997**, *101*, 4265−4275.
(17) Valdés, Á.; Qu, Z.-W.; Kroes, G.-J.; Rossmeisl, J.; Nøskov, J. K. *J. Phys. Chem. C* **2008**, *112*, 9872−9879.
(18) Valdés, Á.; Kroes, G.-J. *J. Phys. Chem. C* **2010**, *114*, 1701−1708.
(19) Zhou, C. Y.; et al. *Chem. Sci.* **2010**, *1*, 575−580.
(20) Matthiesen, J.; Hansen, J. Ø.; Wendt, S.; Lira, E.; Schaub, R.; Lægsgaard, E.; Besenbacher, F.; Hammer, B. *Phys. Rev. Lett.* **2009**, *102*, 226101.
(21) Suzuki, S.; Fukui, K.; Onishi, H.; Iwasawa, Y. *Phys. Rev. Lett.* **2000**, *84*, 2156−2159.
(22) Schaub, R.; Thostrup, R.; Lopez, N.; Lægsgaard, E.; Stensgaard, I.; Nørskov, J. K.; Besenbacher, F. *Phys. Rev. Lett.* **2001**, *87*, 266104.
(23) Brookes, I. M.; Muryn, C. A.; Thornton, G. *Phys. Rev. Lett.* **2001**, *87*, 266103.
(24) Di Valentin, C.; Pacchioni, G.; Selloni, A. *Phys. Rev. Lett.* **2006**, *97*, 166803.
(25) Wendt, S.; Matthiesen, J.; Schaub, R.; Vestergaard, E. K.; Lægsgaard, E.; Besenbacher, F.; Hammer, B. *Phys. Rev. Lett.* **2006**, *96*, 066107.
(26) Li, S. C.; Zhang, Z.; Sheppard, D.; Kay, B. D.; White, J. M.; Du, Y.; Lyubinetsky, I.; Henkelman, G.; Dohnálek, Z. *J. Am. Chem. Soc.* **2008**, *130*, 9080−9088.
(27) Cui, X. F.; Wang, Z.; Tan, S. J.; Wang, B.; Yang, J. L.; Hou, J. G. *J. Phys. Chem. C* **2009**, *113*, 13204−13208.
(28) Acharya, D. P.; Ciobanu, C. V.; Camillone, N.; Sutter, P. *J. Phys. Chem. C* **2010**, *114*, 21510−21515.
(29) Bikondoa, O.; Pang, C. L.; Ithnin, R.; Muryn, C. A.; Onishi, H.; Thornton, G. *Nat. Mater.* **2006**, *5*, 189−192.
(30) Du, Y. G.; Deskins, N. A.; Zhang, Z. R.; Dohnalek, Z.; Dupuis, M.; Lyubinetsky, I. *J. Phys. Chem. C* **2011**, *114*, 17080−17084.
(31) Du, Y. G.; Deskins, N. A.; Zhang, Z. R.; Dohnalek, Z.; Dupuis, M.; Lyubinetsky, I. *J. Phys. Chem. C* **2009**, *113*, 666*i*C671.
(32) Pan, S.; Fu, Q.; Huang, T.; Zhao, A. D.; Wang, B.; Luo, Y.; Yang, J. L.; Hou, J. G. *Proc. Natl. Acad. Sci. U.S.A.* **2009**, *106*, 15259−15263.
(33) Grela, M. A.; Colussi, A. J. *J. Phys. Chem. B* **1999**, *103*, 2614−2619.
(34) Brusa, M. A.; Grela, M. A. *J. Phys. Chem. B* **2005**, *109*, 1914−1918.
(35) Yoshihara, T.; Katoh, R.; Furube, A.; Tamaki, Y.; Murai, M.; Hara, K.; Murata, S.; Arakawa, H.; Tachiya, M. *J. Phys. Chem. B* **2004**, *108*, 3817−3823.
(36) Tang, J. W.; Durrant, J. R.; Klug, D. R. *J. Am. Chem. Soc.* **2008**, *130*, 13885−13891.
(37) Wang, Z.-T.; Du, Y.; Dohnálek, Z.; Lyubinetsky, I. *J. Phys. Chem. Lett* **2010**, *1*, 3524−3529.
(38) Tan, S. J.; Ji, Y. F.; Zhao, Y.; Zhao, A. D.; Wang, B.; Yang, J. L.; Hou, J. G. *J. Am. Chem. Soc.* **2011**, *133*, 2002−2009.
(39) Scheiber, P.; Riss, A.; Schmid, M.; Varga, P.; Diebold, U. *Phys. Rev. Lett.* **2010**, *105*, 226101.
(40) Shin, H.-J.; Jung, J.; Motobayashi, K.; Yanagisawa, S.; Morikawa, Y.; Kim, Y.; Kawai, M. *Nat. Mater.* **2010**, *9*, 442−447.
(41) Lee, J.; Sorescu, D. C.; Deng, X. Y. *J. Am. Chem. Soc.* **2011**, *133*, 10066−10069.
(42) Tan, S. J.; Zhao, Y.; Zhao, J.; Wang, Z.; Zhao, A. D.; Ma, C. X.; Wang, B.; Luo, Y.; Yang, J. L.; Hou, J. G. *Phys. Rev. B* **2011**, *84*, 115418.

(43) Ishibashi, K.-I.; Fujishima, A.; Watanabe, T.; Hashimotoa, K. *J. Photochem. Photobiol., A* **2000**, *134*, 139−142.
(44) Murakami, Y.; Kenji, E.; Nosaka, A. Y.; Nosaka, Y. *J. Phys. Chem. B* **2006**, *110*, 16808−16811.
(45) Murakami, Y.; Endo, K.; Ohta, I.; Nosaka, A. Y.; Nosaka, Y. *J. Phys. Chem. C* **2007**, *111*, 11339−11346.
(46) Thiebaud, J.; Thévenet, F.; Fittschen, C. *J. Phys. Chem. C* **2010**, *114*, 3082−3088.
(47) Diebold, U.; Hebenstreit, W.; Leonardelli, G.; Schmid, M.; Varga, P. *Phys. Rev. Lett.* **1998**, *81*, 405−408.
(48) Shen, Q.; Katayama, K.; Sawada, T.; Yamaguchi, M.; Kumagai, Y.; Toyoda, T. *Chem. Phys. Lett.* **2006**, *419*, 464−468.
(49) Yamakata, A.; Ishibashi, T.; Onishi, H. *J. Phys. Chem. B* **2001**, *105*, 7258−7262.
(50) Onda, K.; Li, B.; Zhao, J.; Jordan, K. D.; Yang, J. L.; Petek, H. *Science* **2005**, *308*, 1154−1158.
(51) Li, B.; Zhao, J.; Onda, K.; Jordan, K. D.; Yang, J. L.; Petek, H. *Science* **2006**, *311*, 1436−1449.
(52) Gundlach, L.; Ernstorfer, R.; Willig, F. *Phys. Rev. B* **2006**, *74*, 035324.
(53) Serpone, N.; Lawless, D.; Khairutdinov, R.; Pelizzetti, E. *J. Phys. Chem.* **1995**, *99*, 16655−16661.
(54) Ji, Y.; Wang, B.; Luo, Y. *J. Phys. Chem. C* **2012**, *116*, 7863−7866.
(55) Anpo, M.; Shima, T.; Kubokawa, Y. *Chem. Lett.* **1985**, *12*, 1799−1802.
(56) Ross, A. B. *J. Phys. Chem. Ref. Data* **1985**, *14*, 1041−1100.